Power-System Ambient-Mode Estimation Considering Spectral Load Properties

Vedran S. Perić, *Student Member, IEEE*, and Luigi Vanfretti, *Member, IEEE*

***Abstract*—Existing mode meter algorithms were derived with the assumption that load variations are accurately represented by white noise or an integral of white noise, which may not be satisfied in actual power systems. This paper proposes a mode meter algorithm which relaxes this assumption by explicitly taking into account spectral load characteristics. These characteristics can be either measured or estimated using the inverse of the existing power system model. The method is developed assuming an autoregressive moving average (ARMA) model of the system and incorporating estimated correlations between loads as inputs and synchrophasor measurements as outputs. Performances of the proposed method are compared with the Yule-Walker and N4SID methods using simulated synchrophasor data obtained from the KTH Nordic 32 test system. Finally, the effects of measurement noise on the proposed method are analyzed, as well as the effects of model uncertainty when the power system model is used to determine spectral load characteristics. It is shown that the proposed algorithm increases accuracy in mode estimates when the loads are described with nonwhite noise.**

***Index Terms*—Forced oscillations, load spectrum, mode estimation, mode meter, synchrophasors.**

I. Introduction

POORLY damped power system oscillations reduce network transfer capacity and decrease security margins [1]–[3]. For accurate real-time monitoring of poorly damped oscillations, different algorithms (usually referred to as *mode estimators*) have been developed [4], [5]. Mode estimators use signals from phasor measurement units (PMUs) which provide time-synchronized voltage and current phasor measurements with high sampling frequency (currently up to 50 or 60 Hz). Mode estimation methods can be broadly classified into two main groups, defined here.

- The first group consists of methods that use transient (large disturbance) system responses. These algorithms have very good performances, but they require existence of transient responses in the system, which makes their application difficult in continuous (near real-time) mode estimation [4], [5].
- The second group consists of methods that perform analysis of ambient responses, usually referred to as *mode meters*. Ambient responses are a result of random load changes and can be observed in all system variables (e.g., voltages, currents, powers, and frequency), even under quasisteady-state operation. Information about system transfer functions, and, consequently, system modes, are contained in the spectrum of ambient responses. This property can be seen as a "coloring" of input noise with the system's transfer functions.

Ambient power system responses were first considered in [6], where an autoregressive model of ambient data was used. This method was later extended to incorporate the autoregressive moving average (ARMA) model [7] and the autoregressive model with spectral analysis [8]. Subspace identification [9]–[11] and frequency-domain decomposition [12] have been also applied for mode estimation in power systems. More information on mode estimation algorithms can be found in [5], [8], [13], and [14].

Ledwich and Palmer show in [15] that it is reasonable to assume that loads at the low voltage level can be represented by integral of Gaussian white noise. However, considering only the transmission network (which is common practice for transmission system operators), aggregated loads at the high voltage level have a spectrum whose distribution is determined by dynamic characteristics of the local distribution and surrounding transmission systems. Further, intrinsic oscillatory behavior of loads (load oscillations) [16], [17] makes spectral load properties even more complex. These considerations highlight that aggregated load spectra cannot be accurately described by a simple function such as white noise or integral of white noise.[1]

Properties of input signals have been included in mode estimation using external probing signals, which are usually based on subspace methods [18]. However, existing mode estimation algorithms that use ambient responses assume that spectral distributions of loads are known in advance and constant, i.e., loads are represented by Gaussian white noise or integral of Gaussian white noise [4], [5]. As explained above, this assumption is very strict and may not be satisfied in real-world power systems [16].

This paper proposes a mode meter algorithm which relaxes this assumption, i.e., the method does not assume any underlying load spectral distribution. This refinement makes mode estimates more accurate and independent of spectral load characteristics. The method assumes that load active and reactive powers are available from PMUs placed directly at the load buses. This assumption, even though not satisfied in present-day

Manuscript received March 09, 2013; revised June 19, 2013; accepted November 09, 2013. Date of publication December 12, 2013; date of current version April 16, 2014. The work of V. S. Perić was supported by the European Commission through an Erasmus Mundus Ph.D. Fellowship. The work of L. Vanfretti was supported by Nordic Energy Research through the STRONg^{2}rid project, the STandUP for Energy collaboration initiative, and Statnett SF, the Norwegian TSO. Paper no. TPWRS-00245-2013.

The authors are with the KTH Royal Institute of Technology, SE-100 44, Stockholm, Sweden.

Color versions of one or more of the figures in this paper are available online at http://ieeexplore.ieee.org.

Digital Object Identifier 10.1109/TPWRS.2013.2292331

[1]The use of integral of white noise as a load model instead of pure white noise introduces one additional pole at the complex plane origin which is visible in the measured signals. The locations of other modes are not changed.

power systems, is expected to be fulfilled in the near future [19]. However, if some signals are not measured directly, they can be reconstructed using the inverse of the existing power system model, providing estimates of the load spectrums and information about the correlation between loads and measured system outputs. The method adopts an ARMA model as an underlying model of the system. Using the estimated correlations and definition of the ARMA model, the problem of mode estimation is formulated as an unconstrained linear least-square problem which can be solved using well-known optimization techniques. The algorithm concurrently uses all available synchrophasor signals from the network, providing a robust estimate of critical system modes.

Performances of the proposed algorithm are evaluated in the presence and absence of forced oscillations which are a result of load oscillations. The results are compared with two mode estimators: the Yule–Walker algorithm, which is widely accepted as a method with good overall performances [5], and the N4SID method as a representative of the group of subspace identification methods [9].

This paper is organized as follows. Section II introduces the power system model used for load spectrum estimation. In Section III, the proposed method for load spectrum estimation is described. In Section IV, the methodology is verified by simulation studies using a KTH Nordic 32 power system model, whereas additional remarks are given in Section V. Conclusions are drawn in Section VI. The Appendix provides detailed derivation of the inverse power system model which is used in Section III.

II. Power System Model

From the system identification and mode estimation viewpoint, it is neither necessary nor feasible to track all changes in the distribution system due to the large number of components and continuous changes in operating conditions. Further, distribution systems are usually radially connected to the transmission system. This makes the identification of oscillatory events originating at the distribution level relatively straightforward (due to their local nature).

Taking into account the aforementioned considerations, the power system model used in this paper describes dynamics of the transmission system with the distribution system represented by active and reactive power injections at all load buses, i.e., distribution system dynamics are not represented explicitly. Ambient responses, which are of interest here, are mainly driven by small perturbations in the network, and therefore associated power system dynamic behavior can be accurately represented by a linear model [1]–[3].

The inputs of the system are defined as loads variations.[2] Responses (outputs) of the system are variables measured by PMUs (voltage, current phasors, and other derived quantities) *excluding* measurements at the load buses. Thus, the power system model can be represented in the state-space form, assuming zero initial conditions, as follows:

$$s\Delta\mathbf{X}(s) = \mathbf{A}\Delta\mathbf{X}(s) + [\mathbf{B}_1\mathbf{B}_2][\Delta\mathbf{U}_1(s)\Delta\mathbf{U}_2(s)]^T \quad (1)$$

$$\Delta\mathbf{Y}(s) = \mathbf{C}\Delta\mathbf{X}(s) + [\mathbf{D}_1\mathbf{D}_2][\Delta\mathbf{U}_1(s)\Delta\mathbf{U}_2(s)]^T \quad (2)$$

[2]It is assumed that all control references in the system are held constant and are therefore not considered as the inputs.

where $\Delta\mathbf{U}_1(s)$ and $\Delta\mathbf{U}_2(s)$ are subvectors of the input vector $\Delta\mathbf{U}(s)$, denoting measured and nonmeasured inputs, respectively. Vector $\Delta\mathbf{X}(s)$ denotes the state vector, and $\Delta\mathbf{Y}(s)$ is a vector of output variables measured by PMUs. Note that some or all inputs can be measured by PMUs, but these signals are not part of the output vector $\Delta\mathbf{Y}(s)$. Matrices $\mathbf{A}, \mathbf{B} = [\mathbf{B}_1\mathbf{B}_2], \mathbf{C}$ and $\mathbf{D} = [\mathbf{D}_1\mathbf{D}_2]$ are system, input, output, and control matrices, respectively.

Using the state space model (1)–(2), the transfer function matrix between loads (at the input) and measured variables (at the output) is computed as follows:

$$\mathbf{H}(s) = \mathbf{C}(s\mathbf{I} - \mathbf{A})^{-1}\mathbf{B} + \mathbf{D}. \quad (3)$$

The complete model of the system can be written in a developed form as

$$\begin{aligned} &H_{11}(s)\Delta u_1(s) + \ldots + H_{1N}(s)\Delta u_N(s) = \Delta y_1(s) \\ &H_{21}(s)\Delta u_1(s) + \ldots + H_{2N}(s)\Delta u_N(s) = \Delta y_2(s) \\ &\quad\vdots \qquad\qquad\qquad \vdots \qquad\qquad \vdots \\ &H_{M1}(s)\Delta u_1(s) + \ldots + H_{MN}(s)\Delta u_N(s) = \Delta y_M(s) \end{aligned} \quad (4)$$

where $\Delta u_i(s)$ and $\Delta y_i(s)$ are the ith elements of the vectors $\Delta\mathbf{U}_1(s)$ and $\Delta\mathbf{Y}(s)$, respectively, and H_{ij} is the element of the $\mathbf{H}$ matrix at position (i, j). N denotes the number of inputs (loads) both measured and not measured, i.e., length of $\mathbf{U}(s)$. M denotes the number of outputs (available PMU measurements and length of $\Delta\mathbf{Y}(s)$). This model can be visually represented as shown in Fig. 1.

Fig. 1 shows that a single output signal can be considered as a sum of N components which are driven by only one load (denoted by x in Fig. 1). The decomposed signals are used in the formulation of the mode estimation method which is presented in Section III.

III. Methodology

The block diagram of the proposed method is depicted in Fig. 2. The method assumes that all inputs (loads) are measured, whereas outputs are arbitrarily chosen in accordance with available PMUs in the system. In the case that some inputs are not measured, these signals are reconstructed using the existing model of the system. The rest of this section describes each step in detail.

A. Data Preprocessing

As the first step in the method, preprocessing aims to remove erroneous data and the mean of the measured signal. Further, the signal is downsampled to 5 Hz in order to improve computational efficiency of the algorithm. More details about preprocessing steps can be found in [16] and [20].

B. Reconstruction of Unavailable Signals and Cross-Correlation Estimation

The second step reconstructs signals of active and reactive load powers which are not available from PMUs. The approach consists of using available information about the system (in this case, the existing power system model) in order to obtain an estimate of the required inputs (loads). This procedure avoids the use of predefined signals (such as Gaussian white noise) for representing the loads.

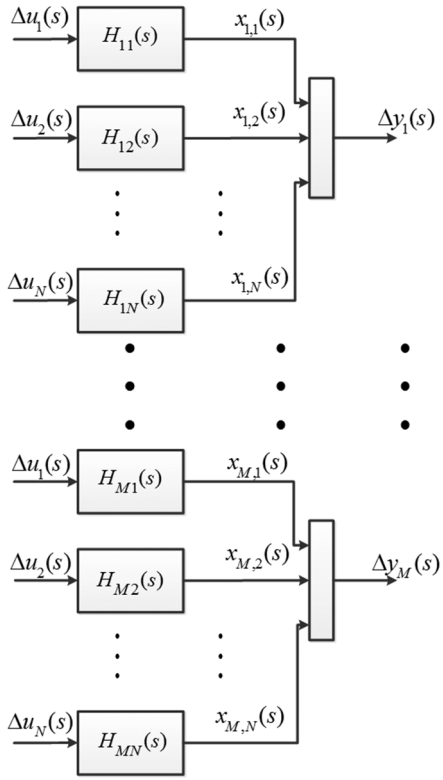

Fig. 1. Model of the power system using loads as inputs and PMU measurements as outputs.

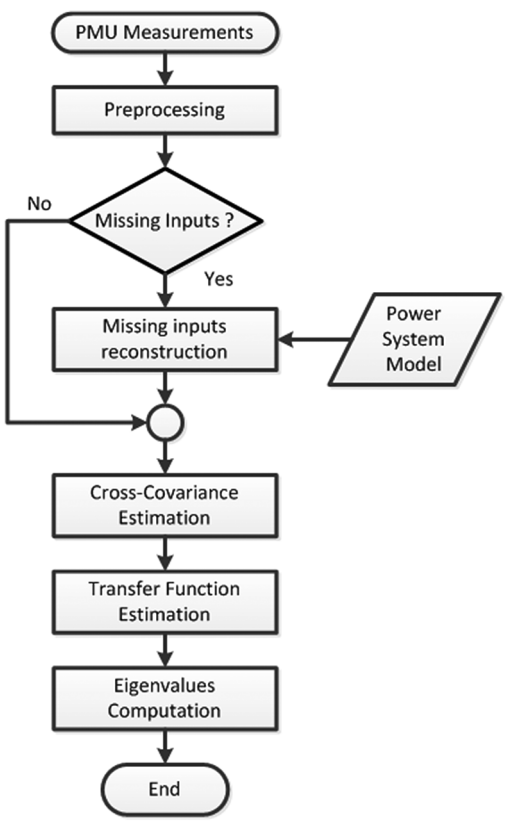

Fig. 2. Global block diagram of the proposed method.

To reconstruct unavailable input signals from the measured outputs, it is necessary to find the inverse system of (1)–(2). The inverse system is the state space system with exchanged roles of the inputs and outputs [21]. In this case, the known outputs are available from synchrophasor measurements and unknown inputs (load variables not measured) need to be computed. The inverse system is given by

$$s\Delta\mathbf{X}(s) = \mathbf{A}'\Delta\mathbf{X}(s) + \mathbf{B}'_1\Delta\mathbf{U}_1(s) + \mathbf{B}'_2\Delta\mathbf{Y}(s) \quad (5)$$

$$\Delta\mathbf{U}_2(s) = \mathbf{C}'\Delta\mathbf{X}(s) + \mathbf{D}'_1\Delta\mathbf{U}_1(s) + \mathbf{D}'_2\Delta\mathbf{Y}(s). \quad (6)$$

Vectors $\Delta\mathbf{X}(s)$, $\Delta\mathbf{U}_1(s), \Delta\mathbf{U}_2(s)$, and $\Delta\mathbf{Y}(s)$ maintain the definition given in Section II. Derivation of the state space matrices of the inverse system ($\mathbf{A}', \mathbf{B}'_1, \mathbf{B}'_2, \mathbf{C}', \mathbf{D}'_1$ and $\mathbf{D}'_2$) are given in the Appendix. Once the inverse system is determined, unknown input signals are computed by time-domain simulation of the linear system (5)–(6).

At the beginning of this section, it was assumed that all input signals are measured or reconstructed. However, cross correlations between inputs and outputs carry all necessary information for mode estimation,[3] as time-domain input signals are not directly used in the proposed mode estimation method. A kth element in the cross-correlation sequence between two signals ($x_i(n)$ and $x_s(n)$) is estimated as follows:

$$r_{is}(k) = \frac{1}{N}\sum_{n=0}^{N-k-1} x_i(n+k)x_s(n). \quad (7)$$

C. Transfer Function Estimation

As described in Section II, one output signal (measurement) is determined by all inputs (loads) in the system. Using the ARMA model formulation, the equations associated with the ith output can be written as [22]

$$\begin{aligned}
x_{i,1}(n) + \sum_{l=1}^{p} a_p(l)x_{i,1}(n-l) &= \sum_{l=0}^{q} b_{i,1}(l)u_1(n-l)\\
x_{i,2}(n) + \sum_{l=1}^{p} a_p(l)x_{i,2}(n-l) &= \sum_{l=0}^{q} b_{i,2}(l)u_2(n-l)\\
&\vdots \qquad\qquad \vdots \qquad\qquad \vdots\\
x_{i,N}(n) + \sum_{l=1}^{p} a_p(l)x_{i,N}(n-l) &= \sum_{l=0}^{q} b_{i,N}(l)u_N(n-l)
\end{aligned} \quad (8)$$

where $x_{i,j}(n)$ is the contribution of the jth input to the ith output at the sample n, whereas p and q are autoregressive and moving average model orders, respectively, with corresponding coefficients $a_p(l)$ and $b_{i,j}(l)$.

In (8), it is assumed that all denominator coefficients ($a_p(l)$) for each transfer function are the same (considering the unique characteristic polynomial of the system).

[3]Autocorrelation is a special case of cross-correlation where both signals are identical.

The sum of all equations associated with the ith output equation (8) leads to

$$x_i(n) + \sum_{l=1}^{p}\left(\sum_{s=1}^{N} a_p(l)x_{i,s}(n-l)\right) = \sum_{l=0}^{q}\sum_{s=1}^{N} b_{i,s}(l)u_s(n-l) \quad (9)$$

and further

$$x_i(n) + \sum_{l=1}^{p}\left(a_p(l)\sum_{s=1}^{N} x_{i,s}(n-l)\right) = \sum_{l=0}^{q}\sum_{s=1}^{N} b_{i,s}(l)u_s(n-l). \quad (10)$$

By multiplying both sides with $x_i(n-k)$ and taking expected values denoted by $E\{\cdot\}$, the following expression is obtained:

$$E\{x_i(n)x_i(n-k)\} + \sum_{l=1}^{p} a_p(l)E\{x_i(n-l)x_i(n-k)\} = \sum_{l=0}^{q}\sum_{s=1}^{N} b_{i,s}(l)E\{u_s(n-l)x_i(n-k)\}. \quad (11)$$

Using the definition of the autocorrelation and cross-correlation sequences and assuming that inputs are wide-sense stationary [22], (11) can be written in compact form as

$$r_{ii}(k) + \sum_{l=1}^{p} a_p(l)r_{ii}(k-l) = \sum_{l=0}^{q}\sum_{s=1}^{N} b_{i,s}(l)r_{is}(k-l) \quad (12)$$

or in equivalent form

$$\sum_{l=1}^{p} r_{ii}(k-l)a_p(l) - \sum_{l=0}^{q}\sum_{s=1}^{N} r_{is}(k-l)b_{i,s}(l) = -r_{ii}(k) \quad (13)$$

where $r_{ii}(k)$ is the autocorrelation sequence of the ith output signal and $r_{is}(k)$ is the cross correlation between the ith output signal and the sth input (load) signal. These correlation sequences are estimated using (7). Note that all signals have zero mean due to the assumption of an underlying linear model and the performed preprocessing steps (Section III). This ensures that covariances and correlations can be used interchangeably.

The same set of equations can be written for all available output signals ($i = 1, \ldots, M$). Further, an arbitrary number of correlation coefficients can be used ($k = 1, \ldots, K$), forming a set of linear $M \cdot K$ equations. By using a sufficient number of autocorrelation and cross correlation elements, it is possible to form an overdetermined system of equations given by (13). The resulting system is linear with unknown ARMA model parameters. ARMA parameters are computed from (13) using least squares or any other linear programming solver [23]. Note that this is an unconstrained linear least-square problem.

TABLE I
DOMINANT MODES OF THE KTH NORDIC 32 TEST SYSTEM

Mode 1		Mode 2	
Frequency(f)	Damping ratio (ξ)	Frequency (f)	Damping ratio (ξ)
[Hz]	[%]	[Hz]	[%]
0.4987	3.5223	0.7322	3.1801

D. Computation of System Eigenvalues

The computed ARMA model parameters define the characteristic polynomial of the system. The roots of the characteristic polynomial are the system poles (eigenvalues) in the z-domain which can be transformed to the s-domain using the well-known transform [1]

$$\mathbf{s} = \boldsymbol{\sigma} + j\boldsymbol{\omega} = \frac{1}{T_s}\ln(\mathbf{z}) \quad (14)$$

where T_s is the signal's sampling period and $\mathbf{z}$ is a vector of computed poles in the z-domain. $\boldsymbol{\sigma}$ and $\boldsymbol{\omega}$ are real and imaginary components of the modes in the s-domain ($\mathbf{s}$), respectively. Once the s-domain modes of the system are calculated, damping ratio of the ith pole (ξ_i) can be easily computed from

$$\xi_i = \frac{-\sigma_i}{\sqrt{\sigma_i^2 + \omega_i}} \quad (15)$$

in order to perform a small-signal stability assessment of the system.

IV. STUDY CASES

The proposed method is demonstrated using the KTH Nordic 32 test system [24]. The system has 44 inputs (22 load buses) and a total of 52 buses where voltage magnitudes are measured. Small-signal stability analysis shows two dominant modes whose properties are given in Table I. Also, study cases are carried out to assess the performance of the proposed method and to compare it with other methods (Yule–Walker and N4SID method, later referred to as conventional methods).

In all studies, a 13-min data window is used for mode estimation (3900 samples obtained after the preprocessing procedure where signal is downsampled to 5 Hz).

The autoregressive model order of the estimated model is chosen to be 25, whereas the moving average order is equal to 2. For the proposed method, 125 elements of the correlation sequences are used ($K = 125$) which corresponds to a 25-s interval with 5-Hz sampling rate. Considering that the system has 52 outputs ($M = 52$), the total number of equations in the unconstrained linear least-square problem is equal to 6500. Statistical properties of the three estimators are evaluated with 1000 independent Monte Carlo simulations.

A. Mode Estimation in the Presence of a Forced Oscillation

The main advantage of the proposed method is that it takes into account properties of the input spectrum. For the sake of simplicity, the most comprehensive nonwhite signals, i.e., white noise with only one permanent oscillation, are used to model load variations. This type of load behavior (sometimes referred to as cyclic load) has been identified in power system literature [25]. It can be caused by some specific industrial processes [26] or intrinsic element properties, such as diesel generators [27].

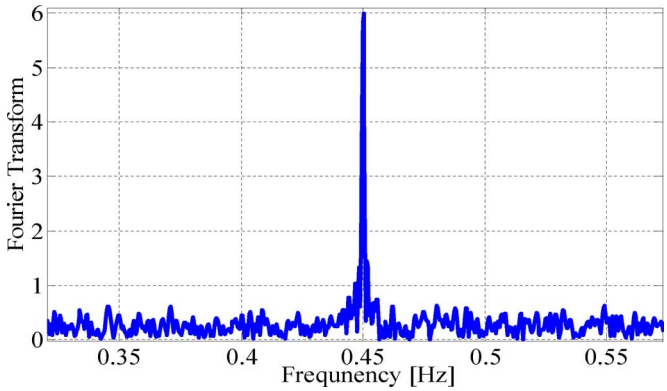

Fig. 3. Fourier transform of the active power signal with a load oscillation at 0.45 Hz.

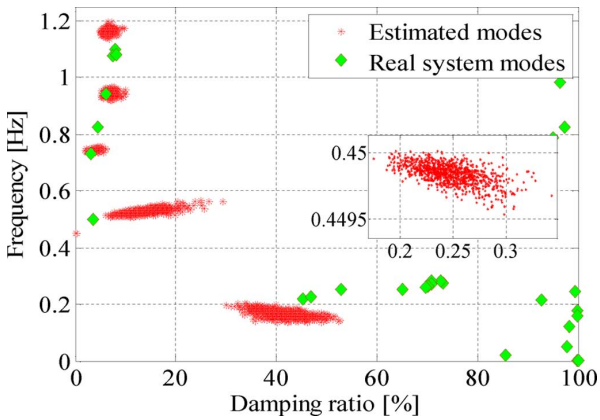

Fig. 4. ARMA 25/2 mode estimation using the Yule–Walker method in the presence of forced oscillations at 0.45 Hz.

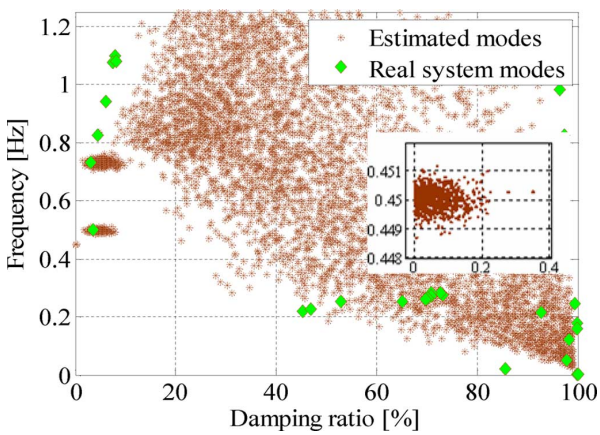

Fig. 5. ARMA 25/2 mode estimation using the N4SID method in the presence of forced oscillation at 0.45 Hz.

This topic has gained more interest in recent time with the deployment of large number of wind turbines which show oscillatory behavior due to mechanical properties of the turbine [28].

In this study, all load signals (active and reactive powers) are modeled by a load oscillation at 0.45 Hz, which is added to a Gaussian white noise with a signal-to-noise ratio of 17 dB (the squared amplitude of the sinusoidal signal component is 25 times smaller than the noise variance). A Fourier transform

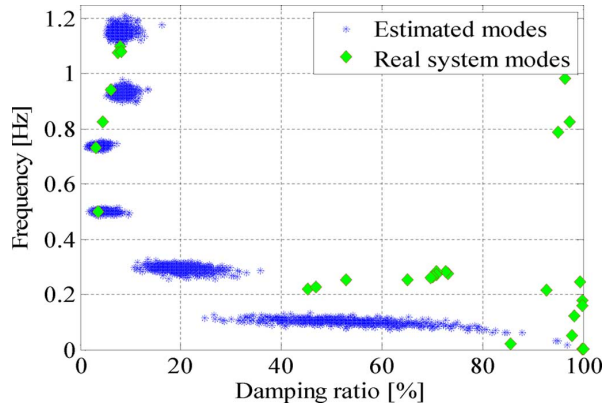

Fig. 6. ARMA 25/2 mode estimation using the proposed method in the presence of forced oscillation at 0.45 Hz.

TABLE II
STOCHASTIC PROPERTIES OF THE ESTIMATION RESULTS IN THE CASE WHERE A FORCED OSCILLATION IS PRESENT IN THE LOAD SIGNALS

Parameters \ Method		Yule-Walker	N4SID	Proposed Method
Mode 1	Mean {f} [Hz]	0.4498	0.4500	0.5009
	Mean {ξ} [%]	0.2470	0.0621	4.8334
	Var {f}	5.745e-9	1.253e-7	2.709e-5
	Var {ξ}	6.798e-4	0.0024	1.4035
Mode 2	Mean {f} [Hz]	0.7445	0.7308	0.7393
	Mean {ξ} [%]	3.7522	4.8403	3.5531
	Var {f}	1.7872e-5	5.154e-5	3.173e-5
	Var{ξ}	0.3640	1.6854	0.6730

of the generated load signal is shown in Fig. 3. Measurement errors are neglected in the simulation studies.

Results of the performed simulations are shown in Figs. 4–6, while numerical results are given in Table II.[4] The obtained results show that both estimators which do not take into account the shape of the load spectrum (Yule–Walker and N4SID) wrongly estimate 0.45 Hz as the most critical electromechanical mode, making the true system mode at 0.5 Hz unobservable. Also, damping of this artificial mode is estimated with very small variance (around 0.001) because the forced oscillation is clearly visible in the spectrum of the measured signals. On the other side, the proposed algorithm correctly discerns the forced oscillation from the *true* system modes in the mode estimation process (mode at 0.45 Hz is not present in Fig. 6). This is possible because information about the load oscillation is extracted from the measured input signal and corresponding correlation sequences.

These results show that the "white noise load" assumption used in the Yule–Walker and N4SID methods is essential for the accurate mode estimation. However, as illustrated in Figs. 4 and 5, this assumption might not hold and, consequently, it will affect results of the mode estimation. On the other hand, the proposed method is not sensitive to the input load spectrum, i.e., it discerns from the main network modes and neglects specific load dynamics.

Another important observation is that when a forced oscillation appears close to one of the true system modes, it deteriorates the accuracy of the Yule–Walker's method for that *true* system

[4]True system modes are given in Table I.

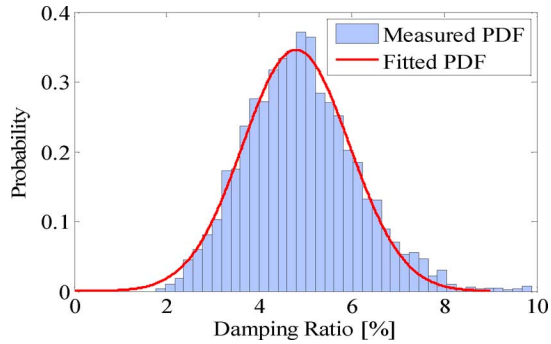

Fig. 7. Probability distribution function (PDF) of the estimates.

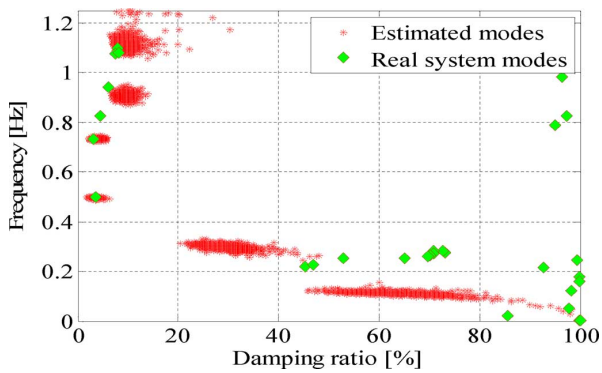

Fig. 8. ARMA 25/2 mode estimation using the Yule–Walker's method with white noise at all inputs.

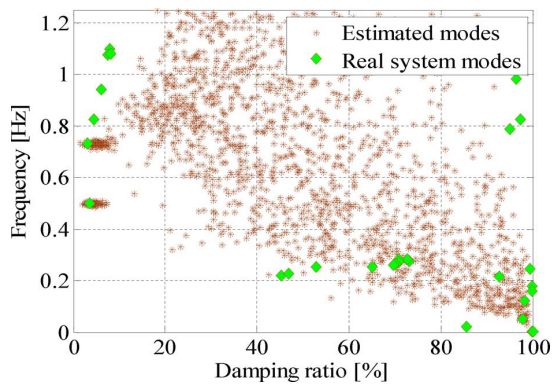

Fig. 9. ARMA 25/2 mode estimation using the N4SID method with white noise at all inputs.

mode. In this case, Mode 1 at 0.4987 Hz is estimated with significantly increased damping and large variance (Fig. 4). In contrast to that, the N4SID method accurately estimates Mode 1 with a variance which is in accordance to general N4SID performance (Fig. 5). Finally, these results show that Yule–Walker shows inferior performance in the presence of the forced oscillation compared with the N4SID method, even though both methods show the drawback of estimating the artificial mode at 0.45 Hz.

In order to determine the distribution of the obtained estimates by the proposed method, a larger number (10 000) of Monte Carlo simulations with randomly generated load variations are performed. It is found that the estimates obey a normal Gaussian distribution function which is shown in Fig. 7.

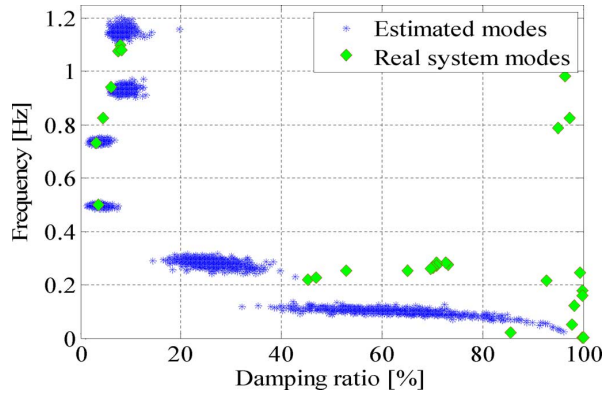

Fig. 10. ARMA 25/2 mode estimation using the proposed method with white noise at all inputs.

TABLE III
STOCHASTIC PROPERTIES OF THE ESTIMATION RESULTS IN THE BASE CASE (LOADS ARE MODELED AS A WHITE NOISE)

Parameters \ Method		Yule-Walker	N4SID	Proposed Method
Mode 1	Mean {f} [Hz]	0.4972	0.4978	0.4966
	Mean {ξ} [%]	3.3081	4.1213	3.8104
	Var {f}	8.8670e-6	1.6260e-5	1.6592e-5
	Var {ξ}	0.2728	0.7942	0.8561
Mode 2	Mean {f} [Hz]	0.7334	0.7309	0.7386
	Mean {ξ} [%]	3.8184	4.7095	3.5497
	Var {f}(10e-5)	1.4072e-5	6.2711e-5	2.3151e-5
	Var{ξ}	0.3563	1.7925	0.5965

B. Mode Estimation With Loads Modeled as Pure Gaussian White Noise

The three mode estimators are compared in the case where input load changes are driven by white noise. This analysis shows that the proposed method provides results with similar accuracy as the conventional methods when their "white noise assumption" is fully satisfied. Results of the three estimators are given in Figs. 8–10, whereas numerical results are summarized in Table III.[5]

It can be noticed that, in this case study, Yule–Walker's method provides slightly better results in terms of variance. This is because the "white noise load" assumption (which is incorporated into Yule–Walker and N4SID methods) is fully satisfied.

On the other hand, the proposed method estimates input spectrums based on measurements leading to higher variance of the estimate. N4SID generally shows inferior performances, both in terms of variance and mean value of the estimate.

In addition, the N4SID method shows very poor results when modes are well damped. Even though these modes are not of interest for mode estimation, the results show that the N4SID algorithm is not suitable for application when more information about well damped modes is required. Figs. 8–10 show one general deficiency of the mode estimation algorithms: closely located modes significantly affect the accuracy of the mode estimates (e.g., modes with frequencies from 0.7 to 1.2 Hz and damping ratio below 15%) [29].

[5]True system modes are given in Table I.

TABLE IV
STOCHASTIC PROPERTIES OF THE ESTIMATION RESULTS WITH MEASURED SIGNALS OF DIFFERENT TYPE

	Paramaters \ Signals	P	Q	P and Q	Currents	Voltage Angles
Mode 1	Mean {f} [Hz]	0.4984	0.4947	0.4957	0.4972	0.4876
	Mean {ξ} [%]	3.4598	4.8100	4.1088	3.687	3.6147
	Var {f}(10e-5)	2.1430	0.9188	2.9195	2.5516	8.6658
	Var {ξ}	1.0031	0.8956	0.3995	1.0146	0.7794
Mode 2	Mean {f} [Hz]	0.7510	0.7396	0.7471	0.7424	0.7364
	Mean {ξ} [%]	4.2281	3.4986	3.9582	4.2144	3.6546
	Var {f}(10e-5)	7.0669	1.0833	4.9610	3.0993	26.605
	Var{ξ}	2.0461	0.6622	0.5883	1.0455	0.7605

This analysis shows the importance of the "white noise load" assumption for conventional methods, whereas the proposed method obtains accurate results regardless of the load spectrum.

C. Mode Estimation Using the Different Types of Synchrophasor Signals

In Sections IV-A and IV-B, voltage magnitude synchrophasor measurements are used with aim to assess performances of the proposed method. However, the method has been derived without assuming any particular output signal type, therefore different signals (such as active and reactive powers, currents, and voltage angles) can also be used for the mode estimation. Table IV shows results of the estimation of the two critical electromechanical modes with measurement signals of different type.

From the results in Table IV, it can be concluded that any type of signal can be successfully used for mode estimation, but the combination of active and reactive power signals provide estimates with slightly lower variance. One reason for this is that number of analyzed signals in this case is larger comparing to other analyzed cases. Voltage angle signals provide high observability of the modes (because of relatively low variance compared to number of used signals), whereas the use of current signals provides less encouraging results.

D. Effects of Measurement Noise on Estimation Accuracy

In order to assess the robustness of the proposed method in the presence of measurement noise, different noise levels are simulated and estimation results are compared with the case where no measurement noise is present. The noise is modeled by adding a Gaussian white noise to the measured signals. The noise-to-signal ratio (NSR) used is defined as a ratio between variance of the measurement noise and variance of the ambient data analyzed. Fig. 11 shows how mean values and variances of the estimates (frequency and damping ratio) change with the different levels of measurement noise. The colored range in Fig. 11 represents ± 0.5 standard deviation of the estimation.

In the case of frequency estimation, the standard deviation is of order 10^{-5}, therefore, this range appears as a thin line in Fig. 11. An important conclusion is that a large amount of noise does not significantly affect the frequency estimation. On the other hand, the estimated damping ratio increases with the increase of the noise level whereas the variance is not significantly increased.

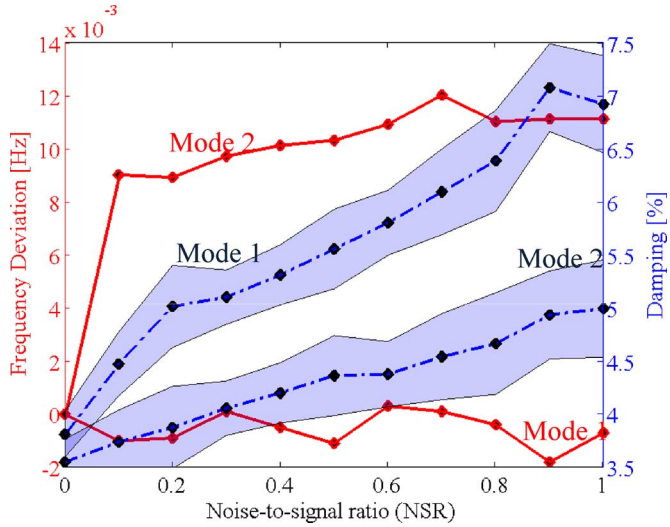

Fig. 11. Effects of measurement noise on frequency and damping estimation.

E. Effects of Load Sensitivity on Mode Estimation

As stated in Section II, the proposed method neglects the behavior of the load, meaning that the method always estimates modes which are associated only to the transmission part of the system (transfer function between load buses and measured signals). Biases introduced by the load behavior can be analyzed using the load model from [2] as follows:

$$P_L = P_0 \left(\frac{V}{V_0}\right)^{\alpha} (1 + K_{pf}\Delta f) \tag{16}$$

$$Q_L = Q_0 \left(\frac{V}{V_0}\right)^{\beta} (1 + K_{qf}\Delta f) \tag{17}$$

where

P_0 and Q_0	initial active and reactive loads;
V_0	voltage magnitude at the initial operating condition;
α and β	coefficients which describe load active and reactive power dependence on voltage variation;
K_{pf} and K_{qf}	load active and reactive power dependence on frequency deviation.

In these studies, typical ranges for the load coefficients are adopted from [2].

Dependence of the location of the first critical mode at 0.5 Hz on different load sensitivity coefficients is shown in Figs. 12 and 13.

It can be concluded that the mode frequency is not significantly affected by load sensitivities, except in the case of reactive power sensitivity on voltage deviation.

System mode damping is more sensitive on load characteristic changes (see Figs. 12 and 13). Based on the presented results, modes of the whole system can be computed from the estimated modes by knowing the model of the loads and using (16) and (17). As can be seen in Figs. 12–13, the uncertainty in load parameters does not introduce significant error in the mode estimation.

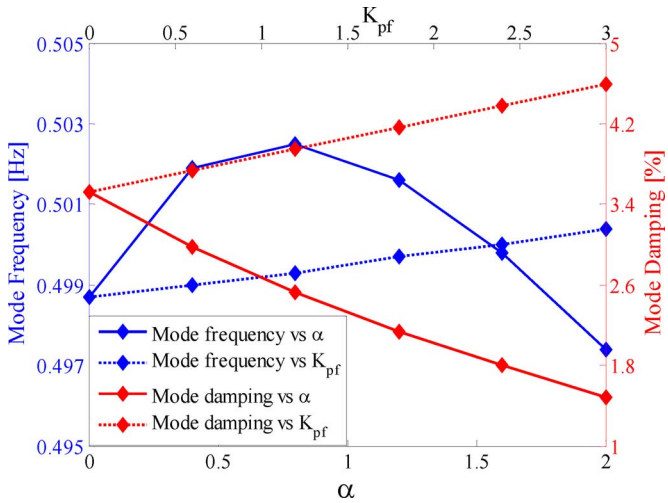

Fig. 12. Sensitivity of the mode location on load active power change caused by variations in voltage and frequency.

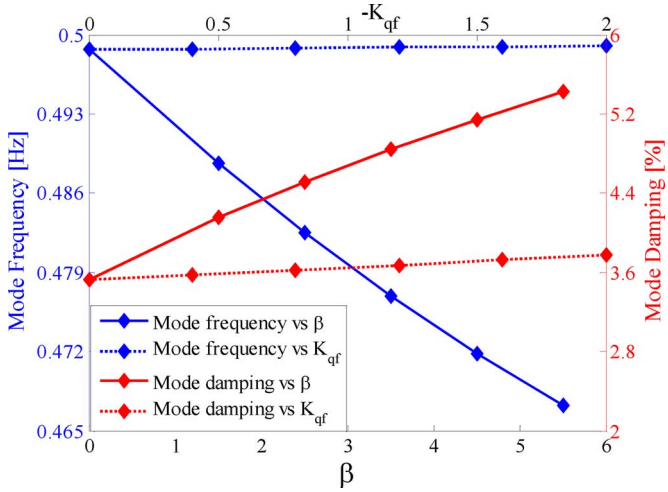

Fig. 13. Sensitivity of the mode location on load reactive power change caused by variations in voltage and frequency.

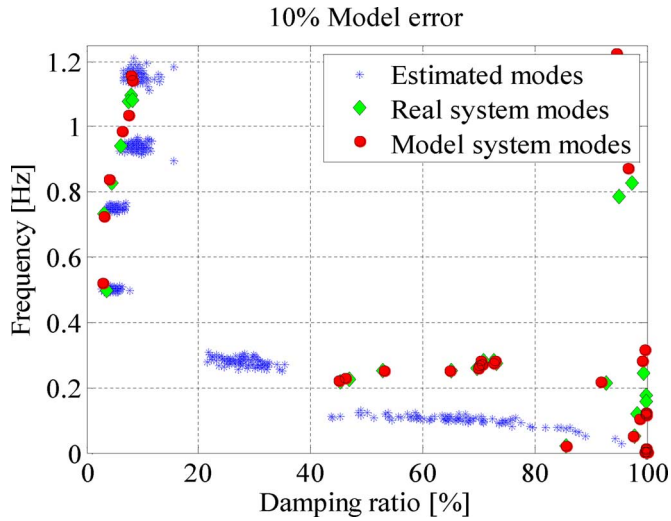

Fig. 14. Mode estimation results using the proposed algorithm with no measured inputs and assumed model with 10% error.

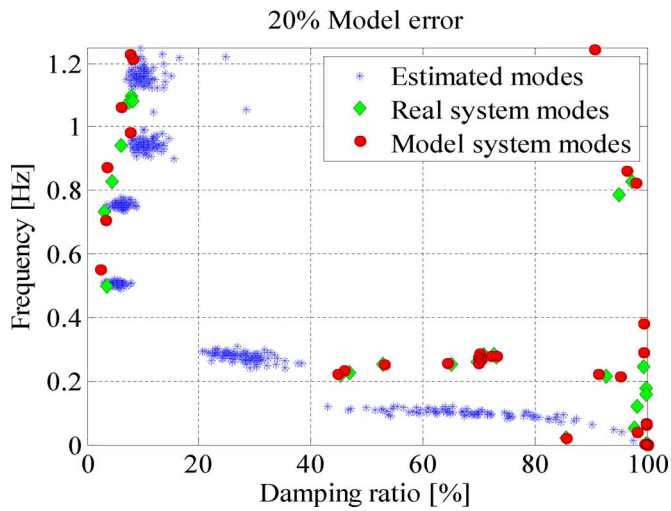

Fig. 15. Mode estimation results using the proposed algorithm with no measured inputs and assumed model with 20% error.

F. Mode Estimation in the Case of Reconstructed Signals

Even though it is envisioned that all buses in the transmission network will be equipped with PMUs in the future, it is necessary to consider a situation where some load buses are not equipped with PMUs or some PMU measurements are not available due to device or communication malfunction. In this regard, the methodology from Section III-B is employed to reconstruct missing measurements at load buses. It is reasonable to expect that a large number of missing load signals and the existing model uncertainty negatively affect the accuracy of the reconstruction procedure. However, even in the case where none of the loads are measured, the procedure provides better estimation of the input–output cross correlations compared with those of any other predefined spectral distribution.

To analyze the method's dependency on model inaccuracy, the generator's inertias and exciters' gains are intentionally changed to model this uncertainty. These model parameters are chosen under assumption that they have a large influence on electromechanical oscillations [1], [3]. In addition, to analyze the dependency on measurement unavailability, none of the input (load) signals are measured and therefore they are all reconstructed using the methodology from Section III-B.

Three test cases are analyzed where generators' inertias and exciters' gains are changed 10%, 20%, and 50% from their original values, respectively. This is done in such way that half of the generators have their original values increased, while the other half have these values decreased. Dominant modes of these modified (uncertain) models are given in Table IV. For each level of model inaccuracy, 100 independent random load variations are simulated and modes are estimated for each one of them. Results from the proposed mode estimation method are presented in Figs. 14–16 and Table V.

Since the inaccurate model is used in the algorithm, the correlation sequences obtained will be imprecise, leading to less reliable but still satisfactory mode estimates which can be seen in Table V. However, the most important property of the estimator, its ability to discern and neglect forced oscillations, is still kept due to the fact that forced oscillations are detected from the input data even with erroneous model parameters such as the ones used in this study cases.

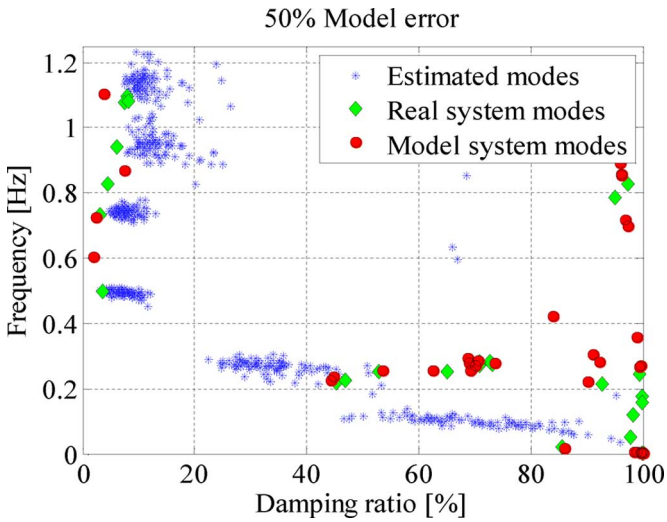

Fig. 16. Mode estimation results using the proposed algorithm with no measured inputs and assumed model with 50% error.

TABLE V
DOMINANT SYSTEM MODES FOR DIFFERENT MODEL UNCERTAINTY LEVELS

Model	Mode 1		Mode 2	
	Frequency (f) [Hz]	Damping (ξ) [%]	Frequency(f) [Hz]	Damping (ξ) [%]
0%	0.4987	3.5223	0.7322	3.1801
10 %	0.5225	2.9569	0.7251	3.1857
20 %	0.5494	2.3961	0.7075	3.3520
50 %	0.6060	1.9014	0.7237	2.3556

TABLE VI
STOCHASTIC PROPERTIES OF THE ESTIMATION RESULTS IN THE CASE WITHOUT MEASURED INPUT SIGNALS AND DIFFERENT MODEL UNCERTAINTY

		10% Model Variation	20% Model Variation	50% Model Variation
Mode 1	Mean {f} [Hz]	0.5022	0.5064	0.4966
	Mean {ξ} [%]	4.5042	5.2139	6.8878
	Var {f}	1.967e-5	2.508e-5	5.197e-5
	Var {ξ}	0.8344	1.0106	2.3343
Mode 2	Mean {f} [Hz]	0.7522	0.7547	0.7427
	Mean {ξ} [%]	4.9322	6.2311	7.4958
	Var {f}	3.318e-5	6.470e-5	1.623e-4
	Var{ξ}	0.6412	0.9853	1.6479

The results in Table V show that, regardless of the model uncertainty, the forced oscillation is not identified as a true system mode. However, model uncertainty has an effect on the accuracy of the estimation process; this can be seen in the mean value and variance of the estimate (larger uncertainty leads to larger bias and variance). Figs. 14–16 also show that the uncertain model does not create bias in the estimated mode frequency but slightly increases value of the estimated damping ratio.

The use of an inaccurate model for distinction between a forced oscillation and a real system mode imposes a possible problem in the case where the model contains no information about the dominant mode. In that case, the real system mode can be interpreted as a forced oscillation and therefore not reported to the operator.

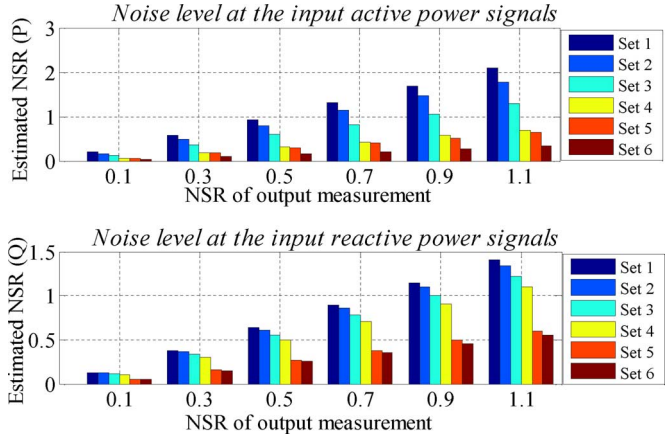

Fig. 17. Errors in load signal estimation by using the inverse power system model caused by output measurement noise.

G. Effects of Measurement Noise on Input Signal Reconstruction

Measurement noise in output signals (which are used for reconstruction of unavailable input signals) corrupts the quality of the estimated input signals. The level of noise produced at the input can be computed using (5) and (6). In the studies performed, a fully accurate model is assumed, meaning that the measurement noise is the only cause of errors for input signal reconstruction.

Different measurement noise levels (up to 1.1 NSR) are simulated and six different sets of output signals are used in the reconstruction process. The selected output signal sets used in the reconstruction process are:

- *Set 1*: Voltage magnitudes in all buses and 60 both active and reactive power flow measurements.[6]
- *Set 2*: Voltage angles in all buses and 60 both active and reactive power flow measurements.
- *Set 3*: Voltage magnitudes and angles in all buses and 80 both active and reactive power flow measurements.
- *Set 4*: Voltage magnitudes and angles in all buses and 80 both active and reactive power flow measurements, as well as 80 current magnitude measurements.
- *Set 5*: Voltage magnitudes and angles in all buses and active and reactive power flow measurements at both ends of all lines in the system.
- *Set 6*: Voltage magnitudes and angles in all buses and active and reactive power flow measurements as well as current magnitude measurements at both ends of all lines in the system.

The computed dependence between noise level in the measured output and resulting noise in the reconstructed input is given in Fig. 17. Two cases are analyzed: the noise level produced at the active power inputs and the noise level at the reactive power inputs.

From Fig. 17, it can be concluded that the first set of measurements provides satisfactory accurate input estimation. This is due to fact that the NSR of the estimated input signal is around 2 for active power and less than 1.5 for reactive power in the case of 1.1 NSR in the output measurements. This proportion approximately holds for all noise levels. A larger number of

[6]There are 80 lines in the system, and PMUs can be installed at both ends.

measured signals reduces the effect of the output noise. In addition, with the large number of measured signals, noise produced at the input has a lower NSR compared to the NSR of the original (output) measurements.

V. Discussion

A. Topology Change

Topology changes may lead to a significant displacement of the modes. Because the time window used for the estimation is in range of 10–15 min, the estimator may not be able to instantaneously calculate new (correct) results after a significant topology change. Instead, the estimated modes have a smooth transition to the correct results.

The ambient system response is present in the measured signals all of the time, whereas topology changes may introduce additional transient responses. Transient response can be used for mode estimation (employing methods that use transient responses) in order to crosscheck the results obtained using an ambient mode estimator.

If the model is used for the input signal reconstruction, it is necessary to update the model after a topology change to reflect the current state of the system. The effects of using an inaccurate model of the system are analyzed in Section IV-F.

B. Computational Complexity

Computational complexity of the proposed method is mainly determined by two steps in the algorithm.

- *Unconstrained linear least-square problem*. The least-square problem is solved in every estimation cycle. The computation time depends on the number of unknown model parameters which is equal to $N \cdot M \cdot q + p$. In the analyzed problem (6500 equations), the required solution time is around 50 s using a MATLAB implementation and a personal computer[7]. The number of unknown parameters is especially sensitive to the order of the numerator (q) in the estimated ARMA model. A high order of the numerator leads to a high order of the least-square problem, which significantly reduces the computational performance of the method.
- *Pseudoinversion* as a part of the input signal reconstruction. This step can take significant computational time in the case where large number of input measurements is missing (up to 7 min for reconstruction of 5000 input signals using a MATLAB implementation and a personal computer). This step is performed only once after the model of the system is updated, therefore, the computational performance is less critical in this case.

All other steps of the methodology (such as the correlation coefficient computation) require negligible computational time and do not affect overall computation performances.

VI. Conclusion

This paper proposes a method for mode estimation using ambient synchrophasor data which relaxes the widely accepted assumption that loads are accurately described by white noise or integral of white noise. The proposed method is founded on the hypothesis that a large number of PMUs is deployed in the system. Despite the fact that this is not the case in present-day power systems, we believe that the sufficient number of PMUs will be deployed in the near future.

The results obtained confirmed that the method correctly exploits information about spectral load properties, enabling the estimator to deal only with *true* system modes. These results indicate that the proposed method will provide more accurate mode estimates in real-life operating conditions where loads can have unpredictable spectral characteristics.

The results obtained suggest that unavailable input signals can be extracted with satisfactory accuracy even with a relatively inaccurate model of the power system. The performed analyses also show that the proposed method provides comparatively accurate results even in the case where the "white noise" load assumption is satisfied, meaning that the proposed method, compared with conventional methods, does not compromise accuracy by any means.

The proposed method correctly estimates modes of the transmission part of the system. If necessary, modes of the overall system (including loads) can be estimated using existing load models to compensate the bias introduced by loads.

The analyses show that the level of measurement noise affects estimation accuracy, particularly damping ratio estimation accuracy. Computational performances predominantly depend on the selected order of the numerator in the estimated ARMA model. A high order can result in unacceptable high dimensions of the least-square problem.

The proposed methodology gives a new perspective to the mode estimation problem. Still, forced oscillations and their effects on mode estimation algorithms in general need to be investigated more thoroughly under real-life conditions. We believe that the best results in practice can be obtained by confronting results from different approaches in an integrated manner; this is a topic for future research. It is also important to investigate new methods for obtaining faster response of the mode estimator in order to make estimation more accurate during transients.

Appendix

An inverse system of the linear dynamical system is defined as a system which, when fed by the output of the original system, at the output gives inputs (excitation) of the original system. It is assumed that the original system is defined by (1)–(2). By using (2), unknown inputs $(\Delta \mathbf{U}_2(s))$ can be expressed as

$$\Delta \mathbf{U}_2(s) = -\mathbf{D}_2^{-1}\mathbf{C}\Delta \mathbf{X}(s) - \mathbf{D}_2^{-1}\mathbf{D}_1\Delta \mathbf{U}_1(s) + \mathbf{D}_2^{-1}\Delta \mathbf{Y}(s) \tag{A1}$$

which represents the output equation of the inverse system. By substituting $\Delta \mathbf{U}_2(s)$ from (A1) into (2), the state space equations of the inverse system are obtained as

$$\begin{aligned} s\Delta \mathbf{x}(s) =& [\mathbf{A} - \mathbf{B}_2\mathbf{D}_2^{-1}\mathbf{C}]\Delta \mathbf{X}(s) + [\mathbf{B}_1 - \mathbf{B}_2\mathbf{D}_2^{-1}\mathbf{D}_1]\Delta \mathbf{U}_1(s) \\ &+ [\mathbf{B}_2\mathbf{D}_2^{-1}]\Delta \mathbf{Y}(s). \end{aligned} \tag{A2}$$

By introducing the following notation:

$$\mathbf{A}' = \mathbf{A} - \mathbf{B}_2\mathbf{D}_2^{-1}\mathbf{C}, \tag{A3}$$

$$\mathbf{B}_1' = \mathbf{B}_1 - \mathbf{B}_2\mathbf{D}_2^{-1}\mathbf{D}_1 \tag{A4}$$

$$\mathbf{B}_2' = \mathbf{B}_2\mathbf{D}_2^{-1} \tag{A5}$$

$$\mathbf{C}' = -\mathbf{D}_2^{-1}\mathbf{C} \tag{A6}$$

$$\mathbf{D}_1' = -\mathbf{D}_2^{-1}\mathbf{D}_1 \tag{A7}$$

$$\mathbf{D}_2' = \mathbf{D}_2^{-1} \tag{A8}$$

[7]Intel i7, 2.7 GHz CPU, and 8 GB of RAM.

a standard state space formulation of the inverse system can be written as

$$s\Delta\mathbf{x}(s) = \mathbf{A}'\Delta\mathbf{x}(s) + \mathbf{B}'_1\Delta\mathbf{u}_1(s) + \mathbf{B}'_2\Delta\mathbf{y}(s) \quad \text{(A9)}$$

$$\Delta\mathbf{u}_2(s) = \mathbf{C}'\Delta\mathbf{x}(s) + \mathbf{D}'_1\Delta\mathbf{u}(s) + \mathbf{D}'_2\Delta\mathbf{y}(s) \quad \text{(A10)}$$

which is the formulation used in (5)–(6).

The number of rows in matrix $\mathbf{D}_2$ has to be greater or equal to the number of columns, and the rank of $\mathbf{D}_2$ must be equal to the number rows (number of unknown input signals). If $\mathbf{D}_2$ is not a square matrix, pseudo-inversion is used, which is defined by

$$\mathbf{D}_2^{-1} = \left(\mathbf{D}_2^T\mathbf{D}_2\right)^{-1}\mathbf{D}_2^T. \quad \text{(A11)}$$

REFERENCES

[1] P. W. Sauer and M. A. Pai, *Power System Dynamics and Stability*. Champaign, IL, USA: Stipes, 2007.

[2] P. Kundur, *Power System Stability and Control*. New York, NY, USA: McGraw-Hill, 1994.

[3] G. Rogers, *Power System Oscillations*. Dordrecht, The Netherlands: Kluwer Academic, 1999.

[4] , A. Messina, Ed., *Inter-area Oscillations in Power Systems: A Nonlinear and Nonstationary Perspective*. Berlin, Germany: Springer-Verlag, 2009.

[5] J. J. Sanchez-Gasca, Ed., "Identification of electromechanical modes in power systems," IEEE Task Force Report, , Special Pub. TP462, 2012.

[6] J. W. Pierre, D. J. Trudnowski, and M. K. Donnelly, "Initial results in electromechanical mode identification from ambient data," *IEEE Trans. Power Syst.*, vol. 12, no. 3, pp. 1245–1251, Aug. 1997.

[7] R. W. Wies, J. W. Pierre, and D. J. Trudnowski, "Use of ARMA block processing for estimating stationary low-frequency electromechanical modes of power systems," *IEEE Trans. Power Syst.*, vol. 18, no. 1, pp. 167–173, Feb. 2003.

[8] D. J. Trudnowski, J. W. Pierre, and N. Zhou, "Performance of three mode-meter block-processing algorithms for automated dynamic stability assessment," *IEEE Trans. Power Syst.*, vol. 23, no. 2, pp. 680–690, May 2008.

[9] N. Zhou, J. W. Pierre, and R. W. Wies, "Estimation of low-frequency electromechanical modes of power systems from ambient measurements using a subspace method," in *Proc. North Amer. Power Symp.*, Oct. 20–21, 2003.

[10] H. Ghasemi and C. Cañizares, "Oscillatory stability limit prediction using stochastic subspace identification," *IEEE Trans. Power Syst.*, vol. 21, no. 2, pp. 736–745, May 2006.

[11] J. Turunen *et al.*, "Comparison of three electromechanical oscillation damping estimation methods," *IEEE Trans. Power Syst.*, vol. 26, no. 4, pp. 2398–2407, Nov. 2011.

[12] G. Liu and V. M. Venkatasubramanian, "Oscillation monitoring from ambient PMU measurements by frequency domain decomposition," in *Proc. IEEE Int. Symp. Circuits Syst.*, May 18–21, 2008, pp. 2821–2824.

[13] D. J. Trudnowski and J. W. Pierre, "Overview of algorithms for estimating swing modes from measured responses," in *Proc. IEEE Power Eng. Soc. General Meeting*, Jul. 26–30, 2009, pp. 1–8.

[14] L. Vanfretti *et al.*, "Application of ambient analysis techniques for the estimation of electromechanical oscillations from measured PMU data in four different power systems," *Eur. Trans. Electr. Power*, vol. 21, no. 4, pp. 1640–1656, May 2011.

[15] G. Ledwich and E. Palmer, "Modal estimates from normal operation of power systems," in *Proc. IEEE Power Eng. Soc. Winter Meeting*, Jan. 23–27, 2000, pp. 1527–1531.

[16] L. Vanfretti *et al.*, "Effects of forced oscillations in power system damping estimation," in *Proc. IEEE Int. Works. App. Meas. Power Syst.*, Sep. 26–28, 2012, pp. 1–6.

[17] Y. Yu *et al.*, "The disturbance source identification of forced power oscillation caused by continuous cyclical load," in *Proc. Int. Conf. Electr. Utility Deregulation and Restructuring and Power Technol.*, Jul. 6–9, 2011, pp. 308–313.

[18] N. Zhou, J. W. Pierre, and D. Trudnowski, "A bootstrap method for statistical power system mode estimation and probing signal selection," in *Proc. IEEE PES Power Syst. Conf. & Expo.*, 29 Oct.–1 Nov. 2006, pp. 172–178.

[19] S. Horowitz, A. G. Phadke, and B. Renz, "The future of power transmission," *IEEE Power Energy Mag.*, vol. 8, no. 2, pp. 34–40, Mar.–Apr 2010.

[20] L. Vanfretti, S. Bengtsson, and J. O. Gjerde, "Preprocessing synchronized phasor measurement data for spectral analysis of electromechanical oscillations in the Nordic grid," *Eur. Trans. Electr. Power.*, to be published.

[21] P. Dorato, "On the inverse of linear dynamical systems," *IEEE Trans. Syst. Sci. Cyber.*, vol. 5, no. 1, pp. 43–48, Jan. 1969.

[22] M. H. Hayes, *Statistical Digital Signal Processing and Modeling*. New York, NY, USA: Wiley, 1996.

[23] D. Bertsimas and J. Tsitsiklis, *Introduction to Linear Optimization*. Belmont, MA, USA: Athena Scientific, 1997.

[24] Y. Chompoobutrgool, W. Li, and L. Vanfretti, "Development and implementation of a Nordic grid model for power system small-signal and transient stability studies in a free and open source software," in *Proc. IEEE Power Eng. Soc. General Meeting*, Jul. 22–26, 2012, pp. 1–8.

[25] J. E. Van Ness, "Response of large power systems to cyclic load variations," *IEEE Trans. Power App. Syst.*, vol. PAS-85, no. 7, pp. 723–727, Jul. 1966.

[26] N. Rostamkolai, R. J. Piwko, and A. S. Matusik, "Evaluation of the impact of a large cyclic load on the LILCO power system using time simulation and frequency domain techniques," *IEEE Trans. Power Syst.*, vol. 9, no. 3, pp. 1411–1416, Aug. 1994.

[27] C. D. Vournas, N. Krassas, and B. C. Papadias, "Analysis of forced oscillations in a multimachine power system," in *Proc. Int. Conf. Contr.*, Mar. 25–28, 1991, pp. 443–448.

[28] X. Liu, D. McSwiggan, T. B. Littler, and J. Kennedy, "Measurement-based method for wind farm power system oscillations monitoring," *IET Renew. Power Gen.*, vol. 4, no. 2, pp. 198–209, Mar. 2010.

[29] D. J. Vowles and M. J. Gibbard, "Illustration of an analytical method for selecting signals and locations for power system modal-estimators," in *Proc. IEEE Power Eng. Soc. General Meeting*, Jul. 25–29, 2010, pp. 1–8.

Vedran S. Perić (S'12) received the M.S. degree in power systems and M.S. degree in power electronics from the University of Novi Sad, Novi Sad, Serbia. He is currently working toward the Ph.D. degree at KTH Royal Institute of Technology, Stockholm, Sweden.

From 2008 to 2011, he was a Research and Teaching Assistant with the University of Novi Sad, Novi Sad, Serbia. His research interests include power system operation and control, and application of phasor measurement units in stability assessment and enhancement.

Luigi Vanfretti (S'03–M'10) received the electrical engineering degree from Universidad de San Carlos de Guatemala, Guatemala City, Guatemala, in 2005, and the M.Sc. and Ph.D. degrees in electric power engineering from Rensselaer Polytechnic Institute, Troy, NY, USA, in 2007 and 2009, respectively.

He was a Visiting Researcher with The University of Glasgow, Glasgow, Scotland, in 2005. He became an Assistant Professor with the Electric Power Systems Department, KTH Royal Institute of Technology, Stockholm, Sweden, in 2010 and was conferred the Swedish title of "Docent" in 2012. He is currently a tenured Associate Professor with the same department. He is Special Advisor in Strategy and Public Affairs for the Research and Development Division of Statnett SF, the Norwegian transmission system operator. His duties include architectural analysis for synchrophasor data transfer, communications, and application systems to be utilized in Smart Transmission Grid applications; as well as providing inputs into R&D strategy development and aiding in the execution of collaborative projects with universities, TSOs, and R&D providers. He is an advocate for free/libre and open-source software. His research interests are in the general area of power system dynamics; while his main focus is on the development of applications of PMU data.

Dr. Vanfretti has served, since 2009, in the IEEE Power Engineering Society (PES) PSDP Working Group on Power System Dynamic Measurements, where he is now Vice-Chair. In addition, since 2009, he has served as Vice-Chair of the IEEE PES CAMS Task Force on Open Source Software. For his research and teaching work toward his Ph.D. degree, he was awarded the Charles M. Close Award from Rensselaer Polytechnic Institute.